Supplementary information

In-vitro and *in-vivo* analyses of the effects of source, length, and charge on the cytotoxicity and immunocompatibility of cellulose nanocrystals

Adam M. Weiss[1,2], Nicholas Macke[2], Yefei Zhang[2], Celine Calvino[2], Aaron P. Esser-Kahn,[2,*] Stuart J. Rowan[1,2,3,*]

[1] Department of Chemistry, University of Chicago
5735 S Ellis Ave., Chicago, IL 60637, United States

[2] Pritzker School of Molecular Engineering, University of Chicago
5640 S. Ellis Ave., Chicago, IL 60637, USA

[3] Chemical and Engineering Sciences, Argonne National Laboratory
9700 Cass Avenue, Lemont, Illinois 60439, United States

* Corresponding author E-mails: stuartrowan@uchicago.edu, aesserkahn@uchicago.edu

Index

Supplementary Methods

FT-IR Spectroscopy. Infrared spectra of unmodified and modified CNCs were recorded on a Shimadzu IR Tracer-100 Fourier Transform-Infrared Spectrometer in attenuated total reflection (ATR) mode. Samples were freeze-dried and placed directly onto the crystal for analysis.

Conductometric Titration. Dispersed solutions of CNCs were titrated using NaOH to quantify carboxylate or sulfate half-ester density on the CNCs. About 30 mg CNCs were dispersed in 50 mL dH_2O. In the case of CNC-COOH samples, the pH was adjusted to pH < 3 using 10 M HCl, and 0.01 M NaOH was added incrementally until pH > 10. In the case of CNC-OSO_3^-, samples, samples were immediately titrated with 0.01 M NaOH in 50 μL increments until the conductivity began to increase. In both cases, the pH and conductivity were recorded at each increment. The quantity of NaOH needed to titrate the carboxylic acid moiteties (pKa ≈ 4.5) was determined by noting the region in the titration curve where conductivity was unchanged and used to quantify the presence of carboxylic acids.[S1] The quantity of NaOH needed to titrate the sulfate half-ester moiteties (pKa ≈ 2.5) was determined by noting the initial region at which the conductivity decreased as sulfates were titrated prior to increasing on account of NaOH addition.[S2]

Zeta Potential. Electrophoretic light scattering (ELS) was performed to determine zeta potential using a Wyatt Möbiuζ DLS/ELS instrument. CNC samples were dispersed at 1 mg/mL by brief ultrasonication in DI water, and measurements were performed immediately after at 25 °C using a laser wavelength of 532 nm. Scattered light was collected at a fixed angle of 163.5°, and each measurement was collected as the average of 4-5 scans. Correlation functions and zeta potential calculations were analyzed using Wyatt Dynamics software.

Thermogravimetric Analysis. The thermal stability of CNC samples was investigated using a TA Instruments Q500 thermogravimetric analyzer (TGA). About 3 mg of each sample

were heated from ambient temperature to 110 °C, held between 110-120 °C for 10 min to remove residual water, and then heated to 600 °C at a heating rate of 10-15 °C/min under a nitrogen atmosphere. The results were analyzed using TRIOS (TA Instruments).

NMR Spectroscopy. CNCs were dispersed at 5 mg/mL in D_2O (~5 mL) and sonicated for 15 min to disperse samples and solubilize any trace components (3 s on/off cycles at 25% power). The CNC dispersions were then ultracentrifugated for 30 min at 10,000 G to precipitate the CNCs, and 1 mL supernatant was collected, passed through a 0.22 μm pore-diameter filter, mixed with 10 μL of a 100 mg/mL maleic acid stock (in D_2O) to achieve a concentration of 1 mg/mL, and analyzed via ^{1}H-NMR. NMRs were conducted at 400 MHz (D1 = 42 s) on a Bruker DRX instrument equipped with a BBO probe using Topspin 1.3. Data were plotted with MestReNova.

WAXS Deconvolution. WAXS data obtained for each of the CNC samples were deconvoluted to a five-term Gaussian fit function (gauss5 function in MATLAB) after subtracting the Kapton tape background, where the Gaussian functions describe the major cellulose 1β peaks of 101, 10$\bar{1}$, 021, and 002 as well as an amorphous background peak. The peaks were centered at the following 2-theta angles (± tolerance), where the location of the amorphous peak was constrained between 18-21° (based on the amorphous cellulose spectrum described previously[S3]):

(1,0,1): 14.9° ± 0.2°

(1,0,$\bar{1}$): 16.5° ± 0.2°

(0,2,1): 20.4° ± 0.2°

(0,0,2): 22.7° ± 0.2°

Amorphous: 19.5° ± 1.5°

In some cases, the tolerance was reduced to better match the fitted curve to the raw spectra. The bandwidth of peaks was estimated according to Scherrer's equation **(S1)** in the Gaussian model,

where τ is the width of the CNCs based on AFM imaging, λ is wavelength of incident X-rays, and θ is the Bragg angle used to determine the peak width at full width, half maximum intensity (β).[S4] Finally, the amplitudes were modulated in an iterative fashion to best match the fitted curve to the raw spectra, and the crystallinity index was calculated by dividing the crystalline area (the area under the 101, 10$\bar{1}$, 021, and 002 peaks) divided by the total area of the fitted Gaussian function.

(S1) $$\beta = \frac{0.9\lambda}{\tau \cos\theta}$$

In-vitro **LDH Assay.** RAW-Blue cells were plated in a 96 well plate at 50,000 cells/well in 180 µL DMEM containing 10% HI-FBS and selective antibiotics. Particle suspensions of 1,000 µg/mL were prepared in endotoxin free water, and 20 µL of each treatment was added in triplicate to the cells. After incubation for 20 h, 100 µL supernatant was collected and assayed using a LDH Cytooxicity Assay Kit (Cayman Chemical) according to the manufacturer's procedure. The absorbance was measured by a Multiskan FC plate reader (Thermo Scientific) at 490 nm.

In-vitro **BrdU Assay.** RAW macrophages were plated in a 96 well plate at 25,000 cells/well in 180 µL DMEM containing 10% HI-FBS and selective antibiotics and incubated undisturbed overnight. Particle suspensions of 100 or 1,000 µg/mL were prepared in endotoxin free water, and 20 µL of each treatment was added in triplicate to the cells. After incubation for 12 h, 20 µL of BrdU reagent was added to each well and incubated for an additional 12 h. Cells were subsequently fixed and BrdU incorporation was assayed using BrdU Cell Proliferation Colorimetric ELISA Kit (Abcam) according to the manufacturer's procedure. The absorbance was measured by a Multiskan FC plate reader (Thermo Scientific) at 450 nm.

In-vitro **Cytokine Assays.** RAW-Blue cells were plated in a 96 well plate at 50,000 cells/well in 180 µL DMEM containing 10% HI-FBS and selective antibiotics and incubated undisturbed overnight. Particle suspensions 1,000 µg/mL were prepared in endotoxin free water,

and 20 μL of each treatment was added in triplicate to the cells. After incubation for 24 h, supernatants were removed, diluted 1:1 with Assay Diluent, and analyzed using Mouse TNF-α and IL-6 ELISA MAX kits (BioLegend) according to the manufacturer's procedure.

Supplementary Results

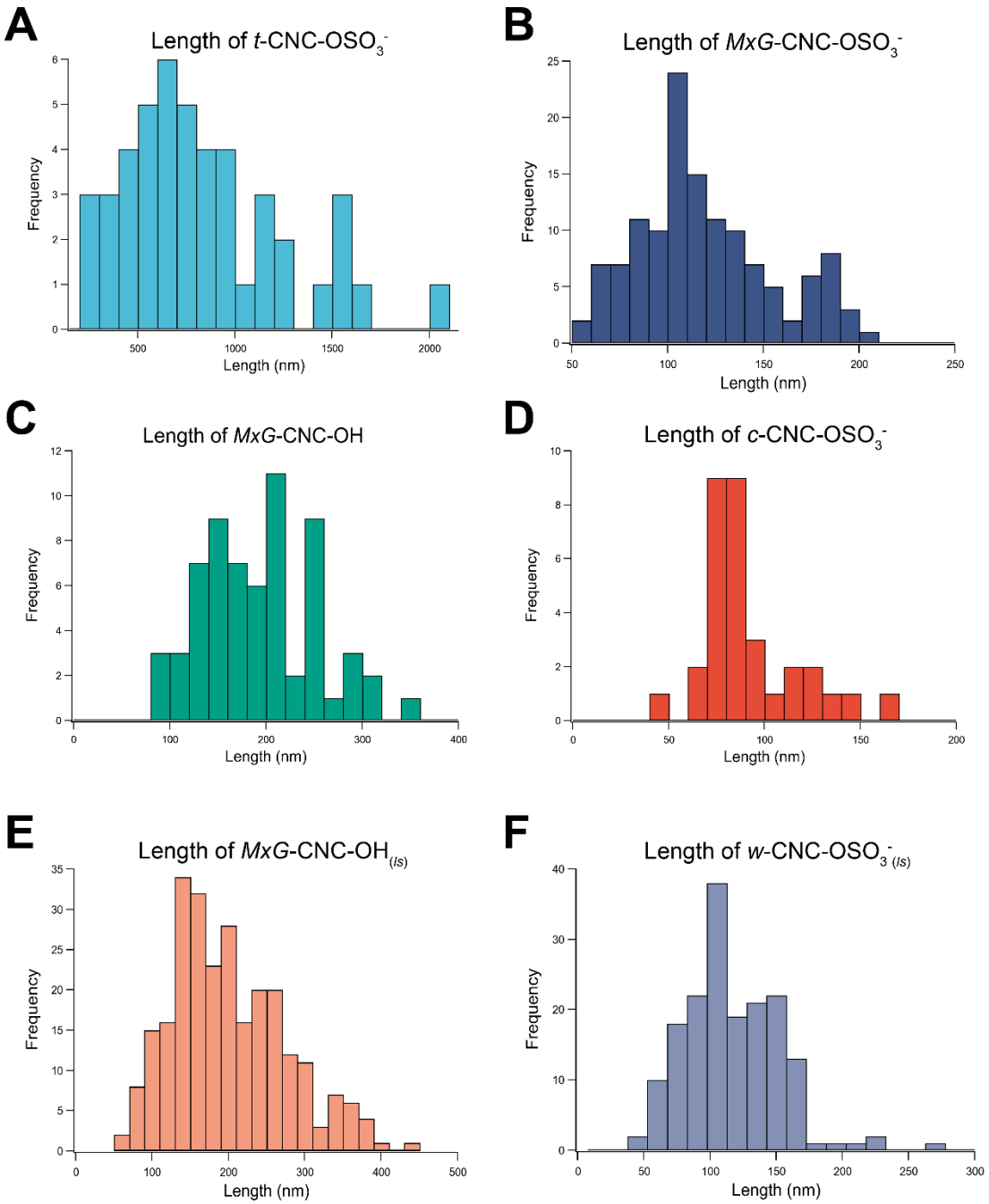

Figure S1: Length distributions of CNC samples obtained from each biosource or large scale production. Samples were imaged using AFM (or TEM for uncharged CNC-OH samples), and the length of individual nanocrystals was evaluated using Gwyddion for SPM (Czech Metrology Institute). At least 50 CNCs were analyzed to determine the length distribution of CNCs.

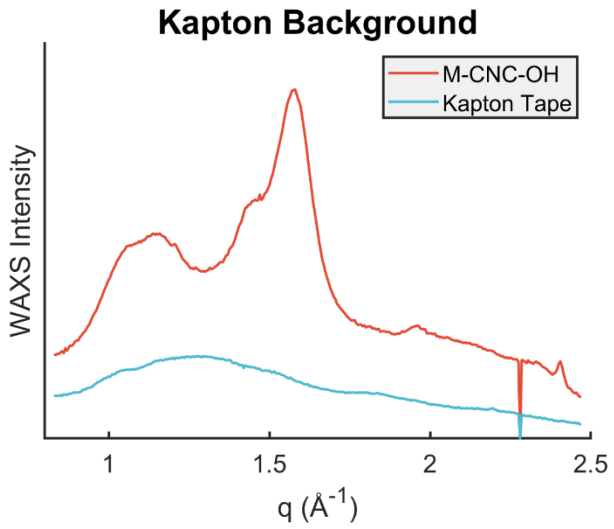

Figure S2: WAXS was conducted by securing CNC samples in a plastic washer using Kapton tape, and the Kapton background spectrum was subtracted prior to determining the crystallinity index of CNC samples (as shown in Figures S3-S7). Here, a representative spectrum of MxG-CNC-OH (prior to background subtraction) and Kapton spectrum are shown for reference.

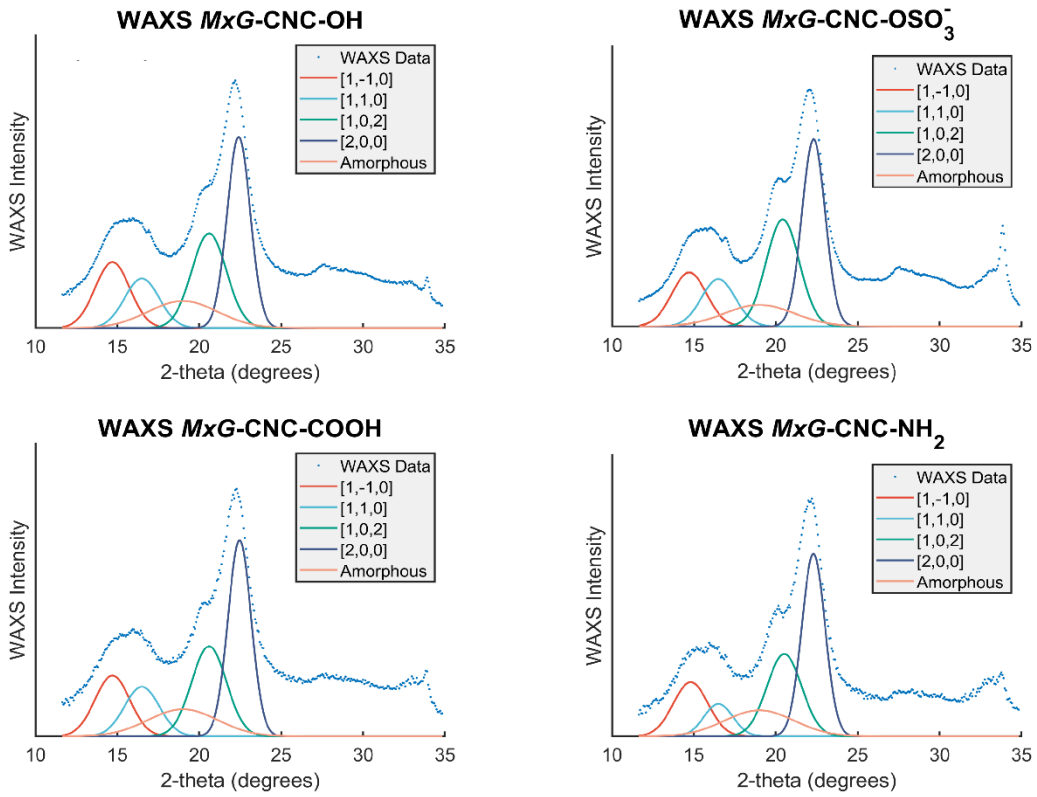

Functionalization	CI
MxG-CNC-OH	86%
MxG-CNC-COOH	86%
MxG-CNC-NH_2	85%
MxG-CNC-OSO_3^-	88%

Figure S3: WAXS diffraction patterns of *MxG* CNC samples showing the peak deconvolution used to determine the crystallinity index (CI) of samples. The crystallinity index was calculated by dividing the amorphous peak area by the total area of the fitted function.

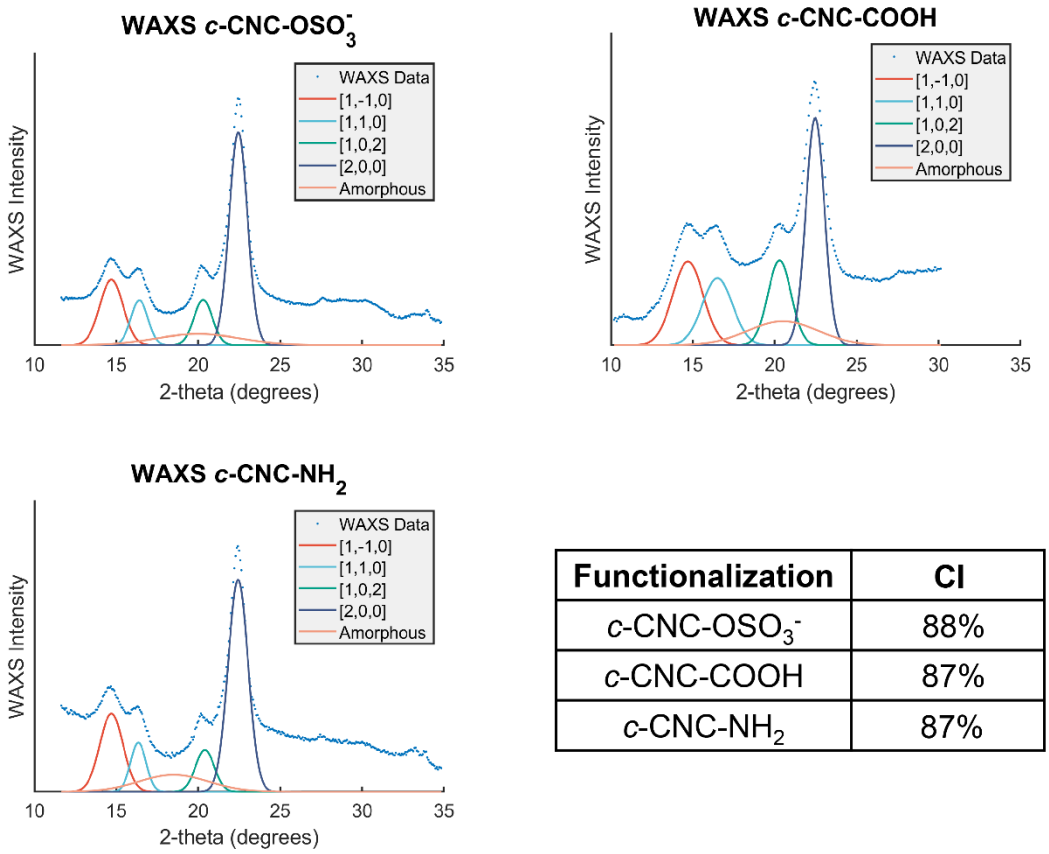

Functionalization	CI
c-CNC-OSO_3^-	88%
c-CNC-COOH	87%
c-CNC-NH_2	87%

Figure S4: WAXS diffraction patterns of cotton CNC samples showing the peak deconvolution used to determine the crystallinity index (CI) of samples. The crystallinity index was calculated by dividing the amorphous peak area by the total area of the fitted function.

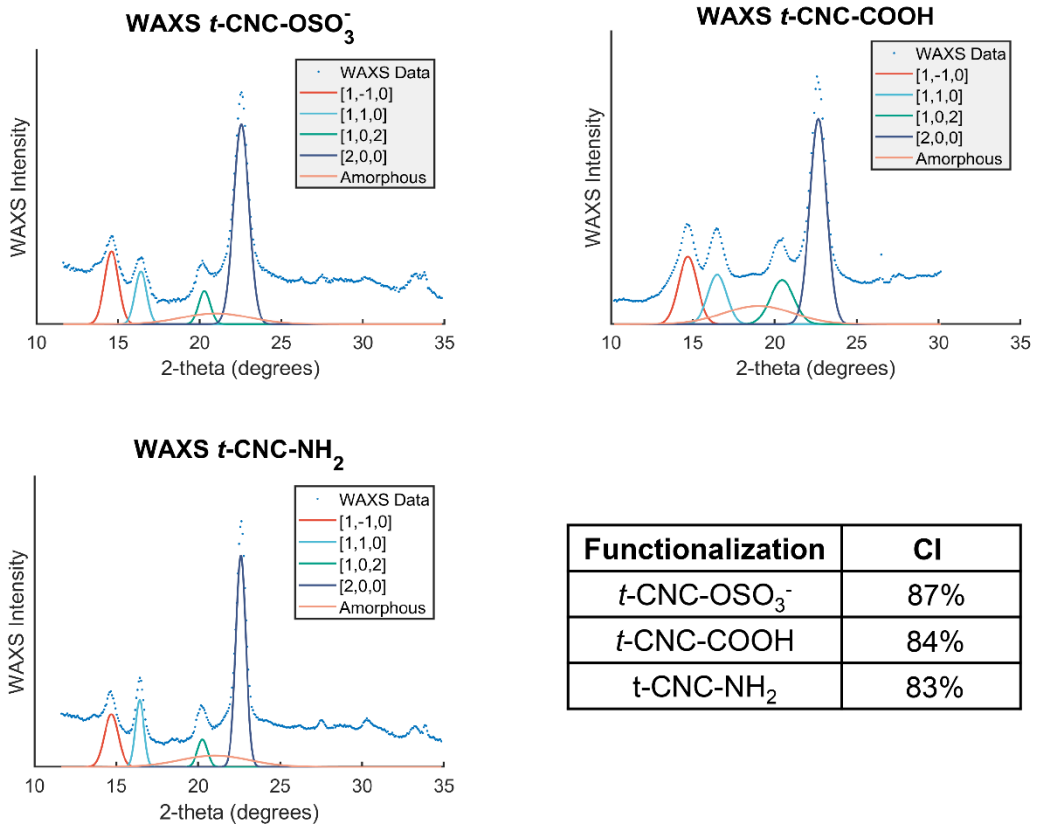

Functionalization	CI
t-CNC-OSO_3^-	87%
t-CNC-COOH	84%
t-CNC-NH_2	83%

Figure S5: WAXS diffraction patterns of tunicate CNC samples showing the peak deconvolution used to determine the crystallinity index (CI) of samples. The crystallinity index was calculated by dividing the amorphous peak area by the total area of the fitted function.

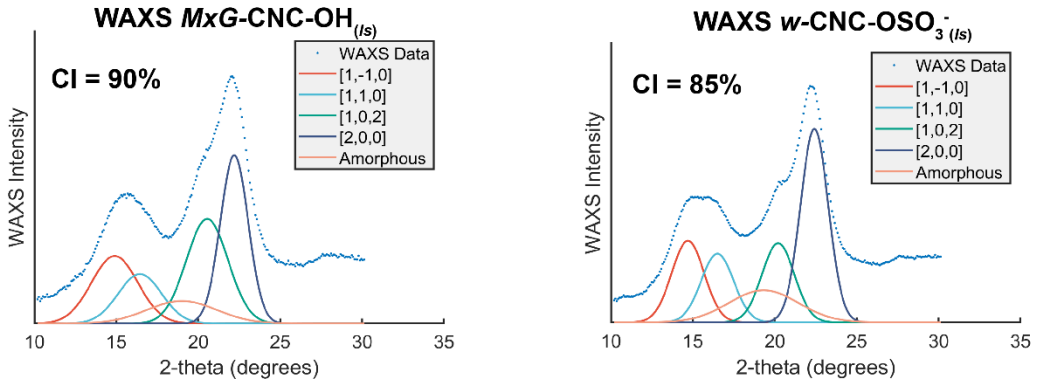

Figure S6: WAXS diffraction patterns of commercial CNC samples showing the peak deconvolution used to determine the crystallinity index (C.I.) of samples. The crystallinity index was calculated by dividing the amorphous peak area by the total area of the fitted function.

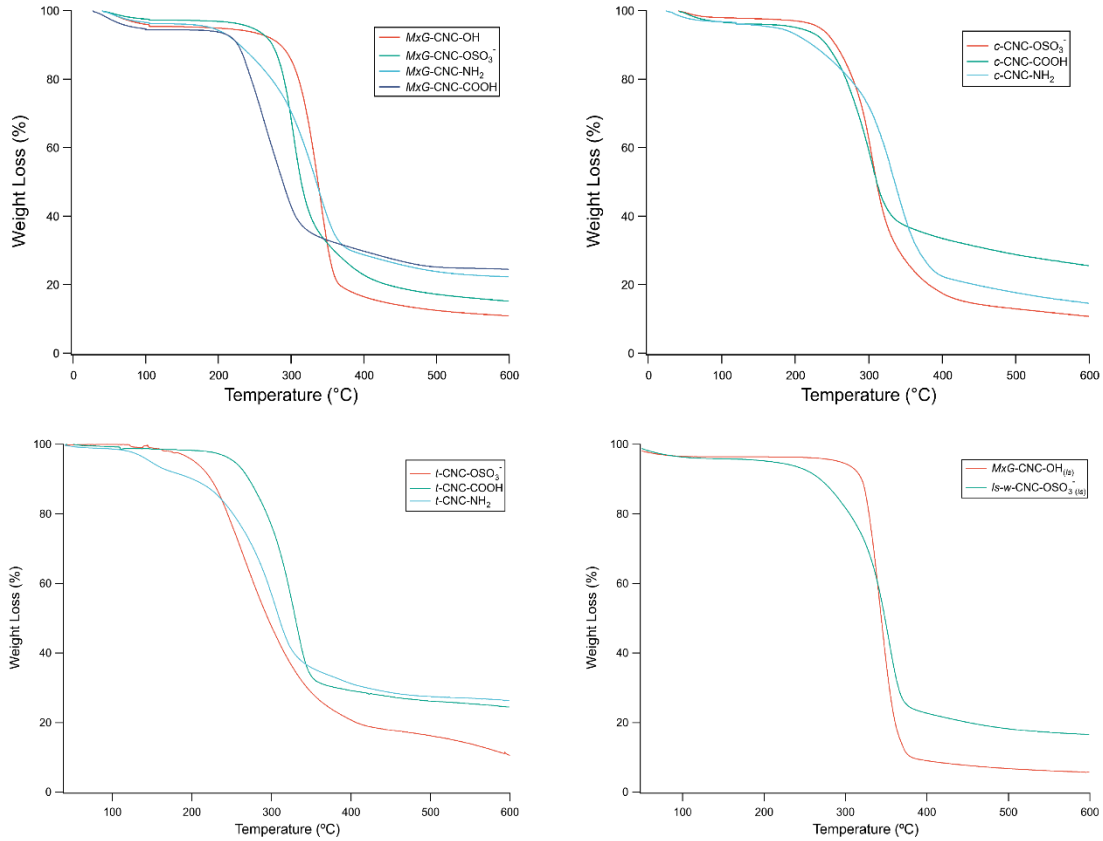

Figure S7: Thermogravimetric analysis (TGA) of CNCs with different source and functionality was conducted by heating the CNCs at 10-15 °C/min and measuring the weight loss due to thermal decomposition. Sulfated CNCs have a characteristic decrease in the decomposition temperature relative to unfunctionalized CNCs. Amine-functionalized CNCs have a characteristic small amount of decomposition between 200-300°C. TEMPO-oxidized CNCs have a characteristic increase in residual mass relative to other samples.

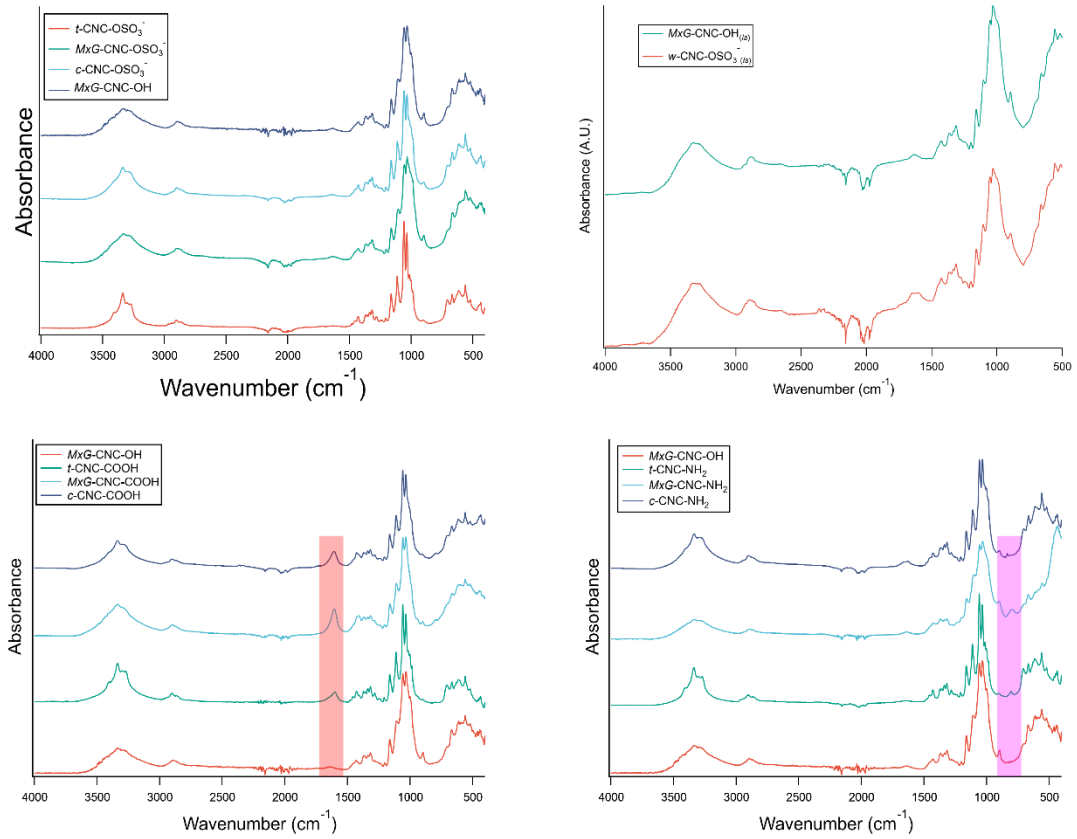

Figure S8: FT-IR of dried CNC samples was conducted to assess chemical groups present in isolated and functionalized materials. TEMPO-oxidized CNCs (CNC-COOH) have a characteristic strong carboxylate peak at ~1600 cm^{-1} (red) while amine-functionalized CNCs (CNC-NH_2) have a characteristic weak amine wag peak at ~800 cm^{-1} (pink).

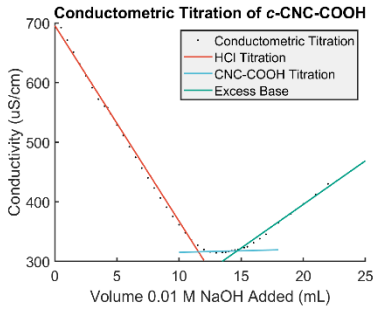

Mass CNCs	20.0 mg
Intercept 1	17.08 mL
Intercept 2	18.91 mL
[CNC-COOH]	920 mmol/kg

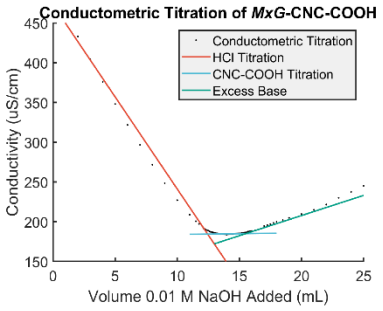

Mass CNCs	30.0 mg
Intercept 1	12.45 mL
Intercept 2	15.53 mL
[CNC-COOH]	1030 mmol/kg

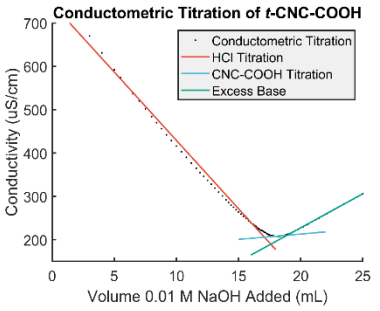

Mass CNCs	23.9 mg
Intercept 1	11.56 mL
Intercept 2	14.68 mL
[CNC-COOH]	1300 mmol/kg

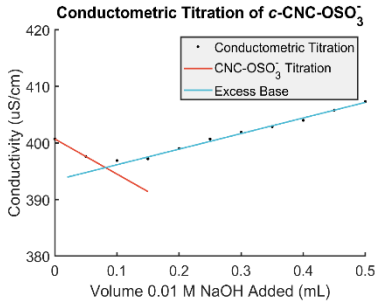

Mass CNCs	44.0 mg
Intercept	0.0815 mL
[CNC-OSO_3^-]	27.2 mmol/kg

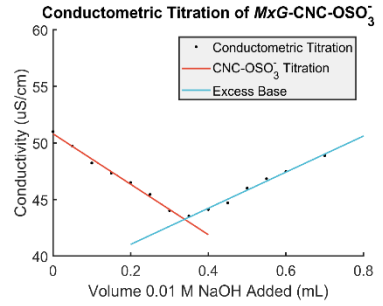

Mass CNCs	44.4 mg
Intercept	0.3390 mL
[CNC-OSO_3^-]	113 mmol/kg

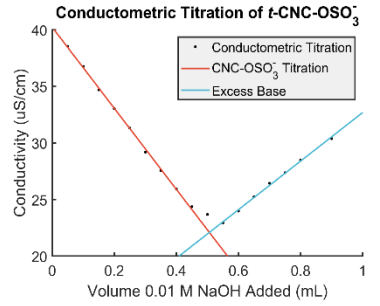

Mass CNCs	30.0 mg
Intercept	0.5061 mL
[CNC-OSO_3^-]	169 mmol/kg

Figure S9: CNCs containing carboxylic acid or sulfate half-ester modifications were acidified and subsequently titrated using 0.01 M NaOH. Conductivity was assayed throughout the titration to determine and quantify the presence of carboxylate or sulfate half-ester moieties on the CNCs. The region in which conductivity does not change corresponds to titration of carboxylic acids, while the initial decrease in conductivity corresponds to the titration of sulfate half-esters.

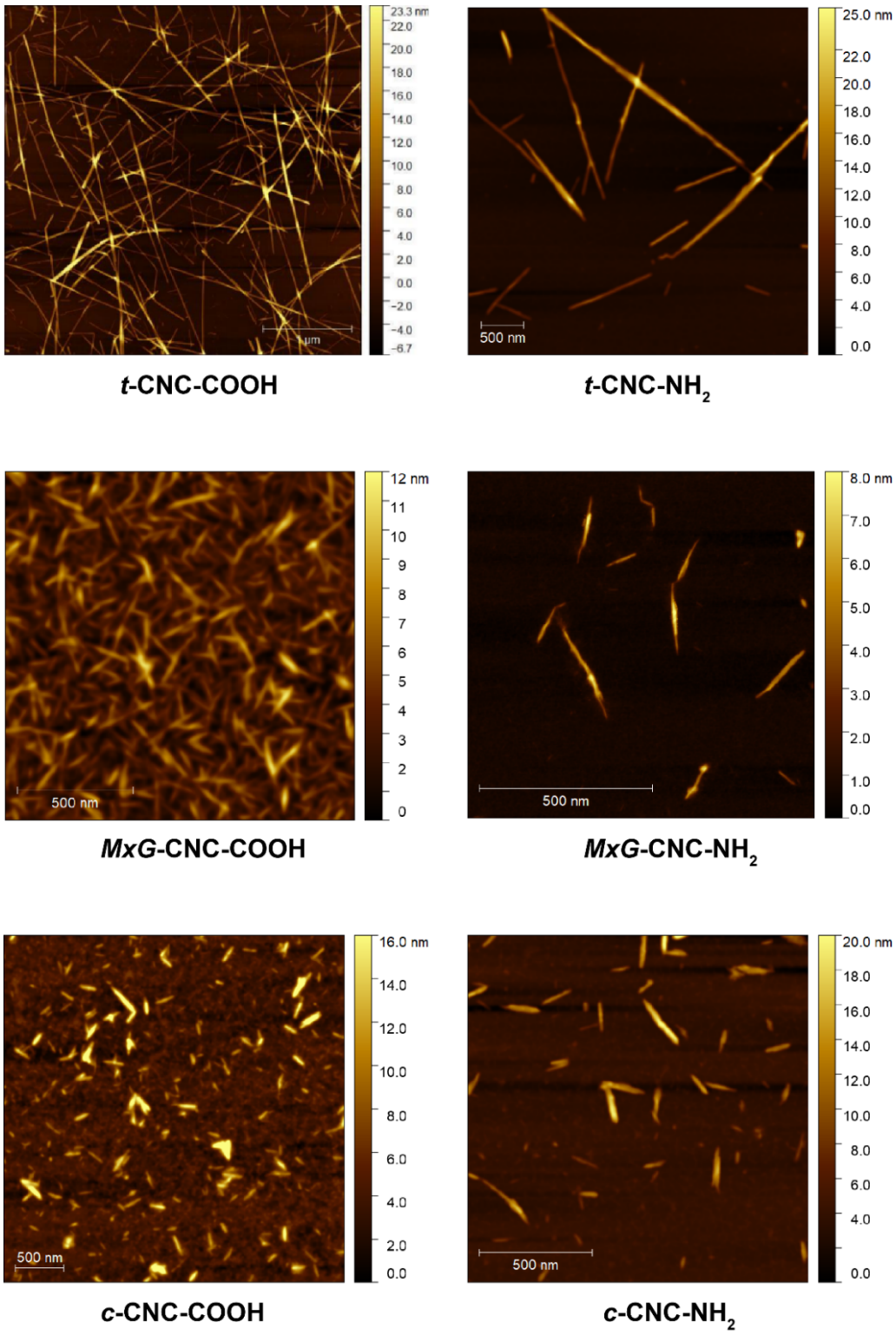

Figure S10: AFM images of carboxylic acid and amine-functionalized CNC were collected to validate that morphology was not altered after functionalization. For imaging, samples were drop cast from a dilute aqueous solution onto a poly-lysine coated mica substrate.

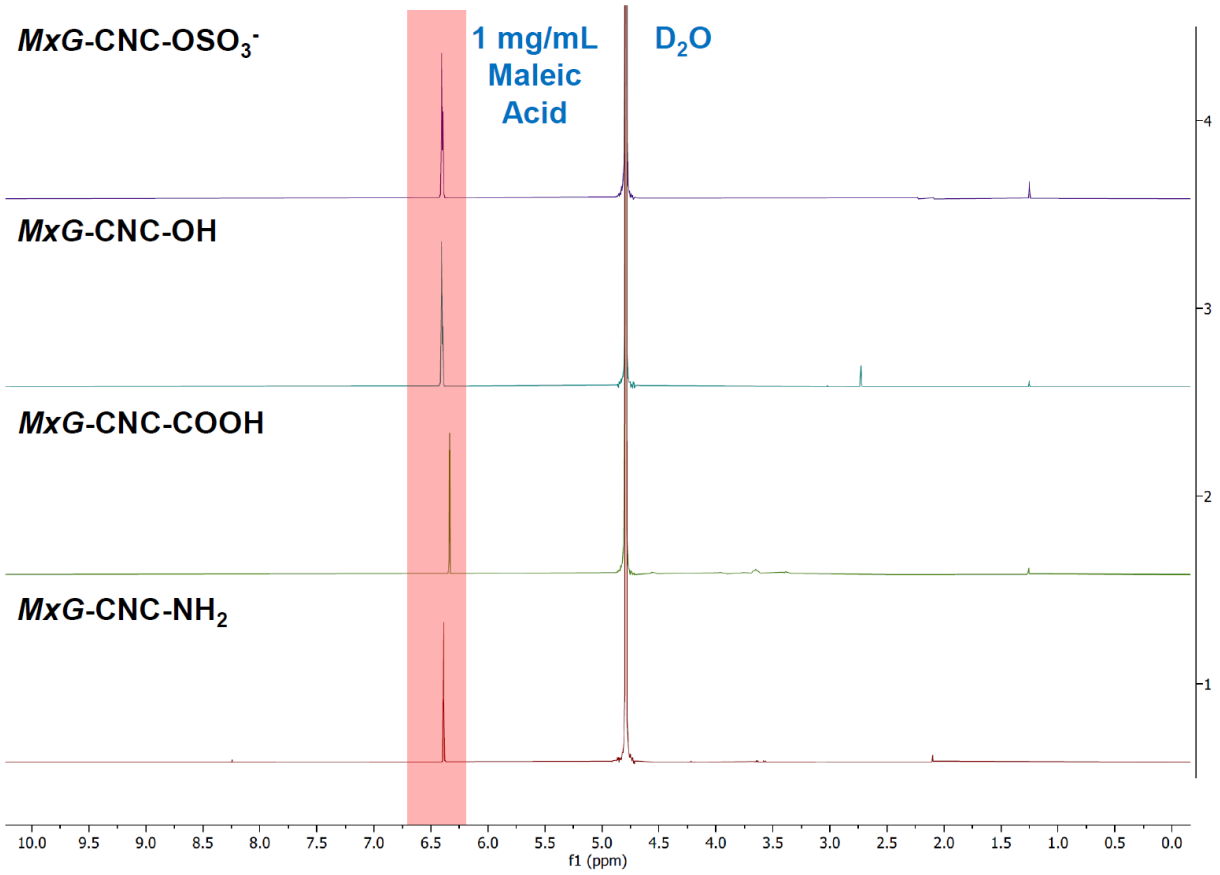

Figure S11: To confirm the presence or absence of lignin or hemicellulose after isolation and functionalization, a subset of the CNCs were dispersed at 5 mg/mL by sonication in D_2O to solubilize any contaminants. CNCs were then removed by ultracentrifugation and filtration, and the supernatant was analyzed by ^{1}H-NMR using maleic acid as an internal standard to semiquantitatively analyze any contaminant groups. The materials were confirmed free of contaminants in the mmol contaminant/g CNC range.

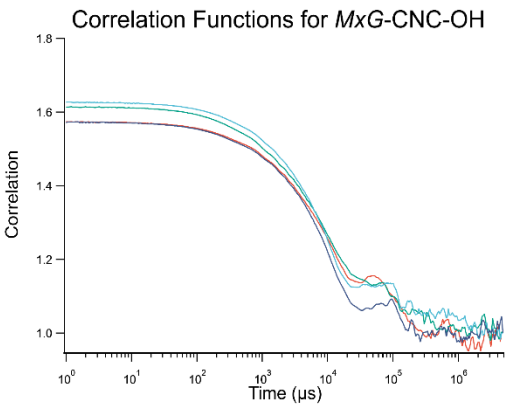

T1	-16.16 mV
T2	-15.94 mV
T3	-16.10 mV
T4	-16.89 mV
Average	-16.3±0.4 mV

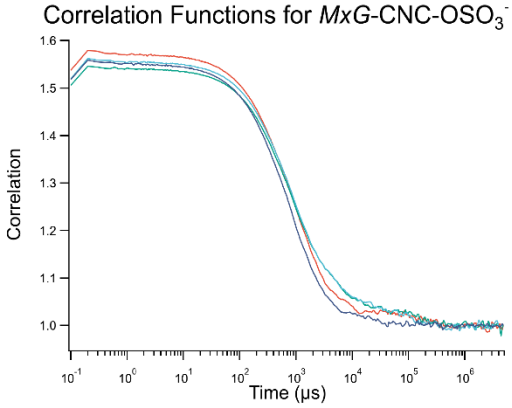

T1	-18.52 mV
T2	-17.54 mV
T3	-19.21 mV
T4	-20.65 mV
Average	-19.0±1.3 mV

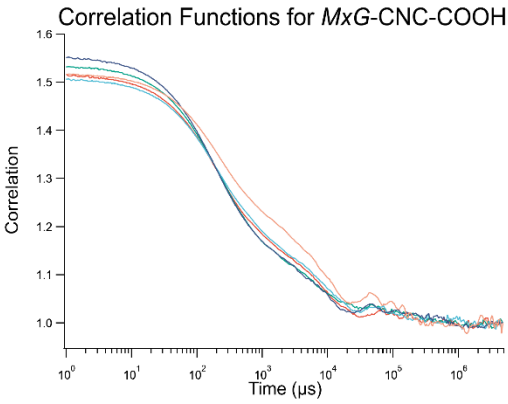

T1	-49.60 mV
T2	-59.41 mV
T3	-51.59 mV
T4	-51.53 mV
T5	-52.59 mV
Average	-52.9±3.8 mV

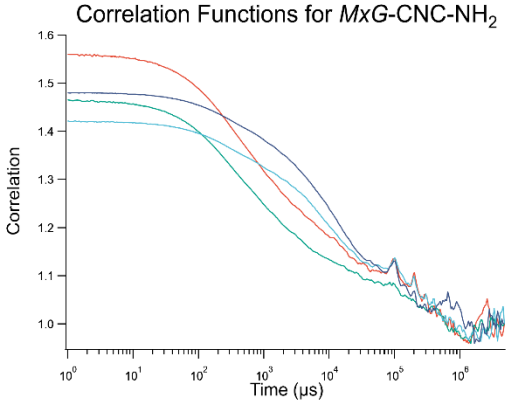

T1	32.91 mV
T2	21.93 mV
T3	24.87 mV
T4	14.93 mV
Average	23.7±7.4 mV

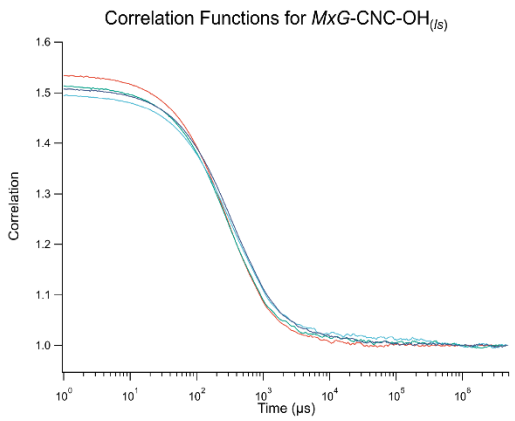

T1	-22.00 mV
T2	-14.47 mV
T3	-17.61 mV
T4	-16.69 mV
Average	-17.7±3.2 mV

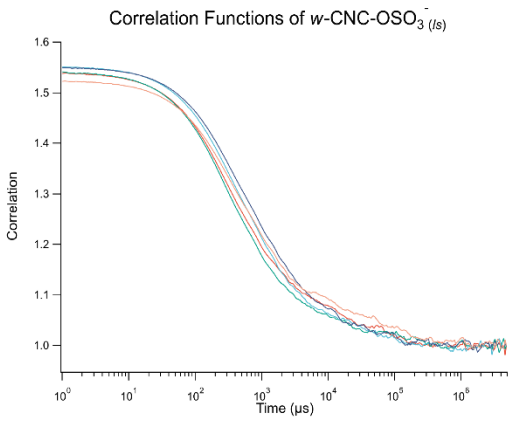

T1	-26.10 mV
T2	-23.69 mV
T3	-26.49 mV
T4	-26.82 mV
T5	-28.13 mV
Average	-26.2±1.6 mV

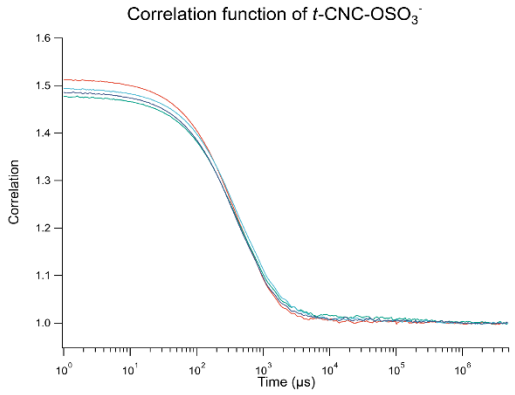

T1	-26.66 mV
T2	-27.67 mV
T3	-28.84 mV
T4	-26.39 mV
Average	-27.4±1.1 mV

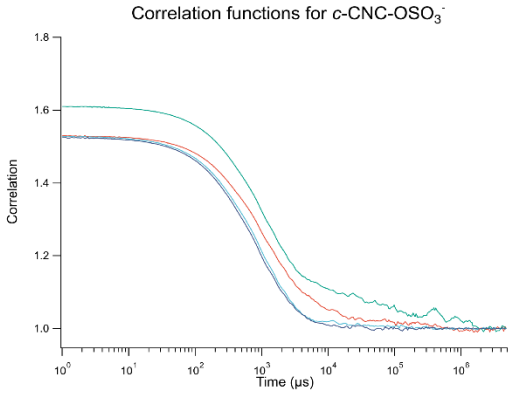

T1	-16.45 mV
T2	-16.07 mV
T3	-16.59 mV
T4	-16.10 mV
Average	-16.3±0.3 mV

Figure S12: Correlation functions obtained and zeta potentials calculated through electrophoretic light scattering experiments. All experiments were conducted five times at 1 V, and outlying correlation functions were removed to obtain the average datasets.

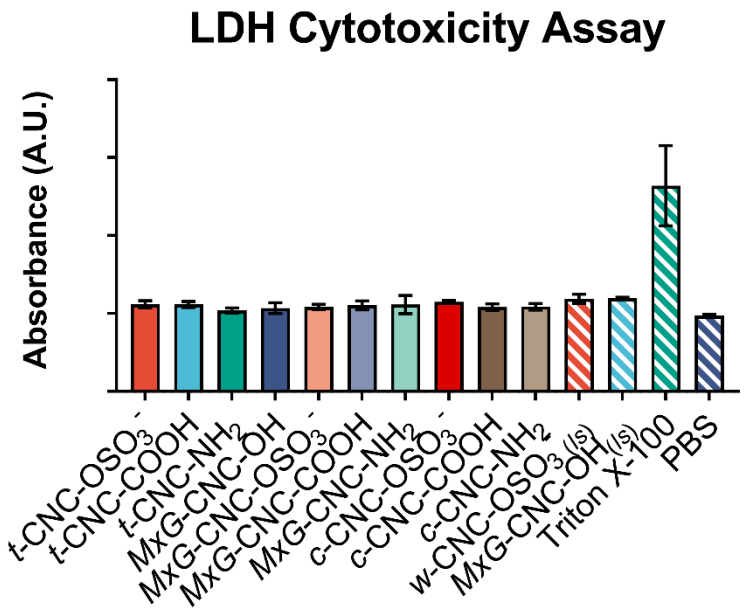

Figure S13: LDH Cytotoxicity Assay was used as a secondary method to measure cytotoxicity induced by CNCs on RAW-Blue cells. CNCs were incubated with cells for 24 h prior to analysis.

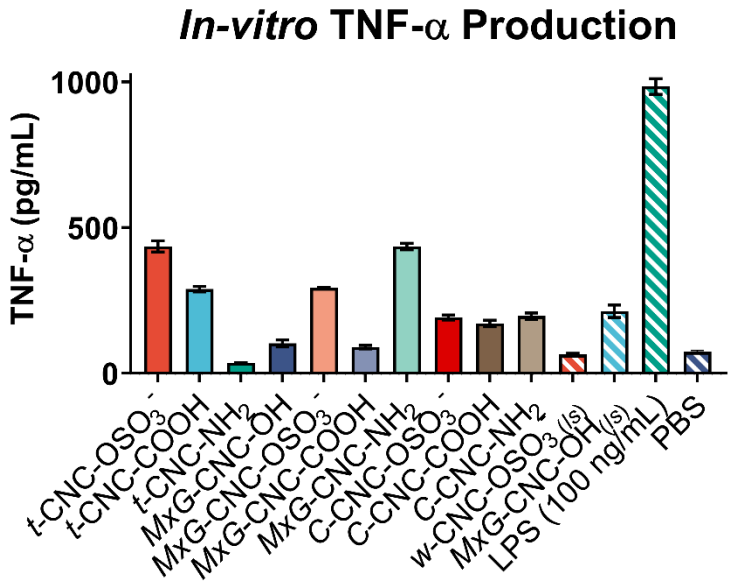

Figure S14: TNF-α ELISA Assay of RAW-Blue supernatant after incubation for 24 h with CNCs indicates a low-level nonspecific inflammatory response to CNCs independent of size or charge.

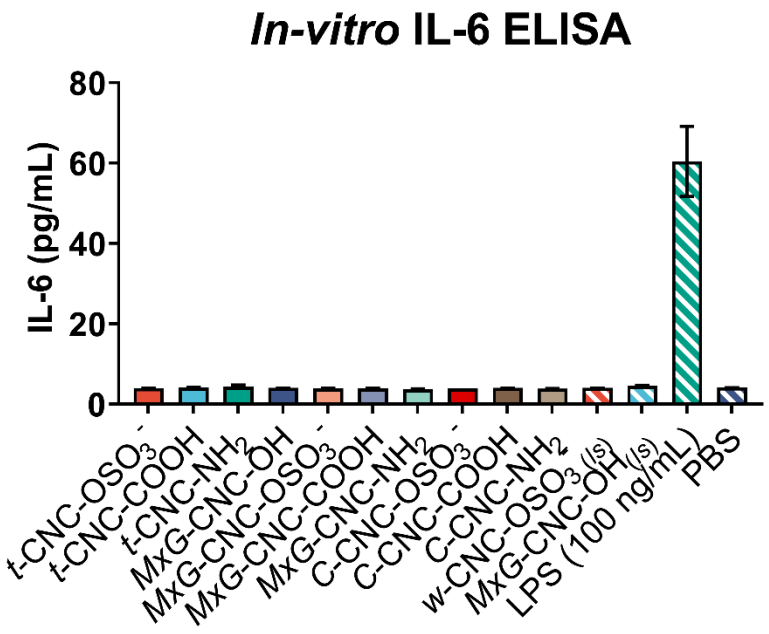

Figure S15: IL-6 ELISA Assay of RAW-Blue supernatant after incubation for 24 h with CNCs indicates absence of a pro-inflammatory IL-6 response resulting from charge or size of CNCs.

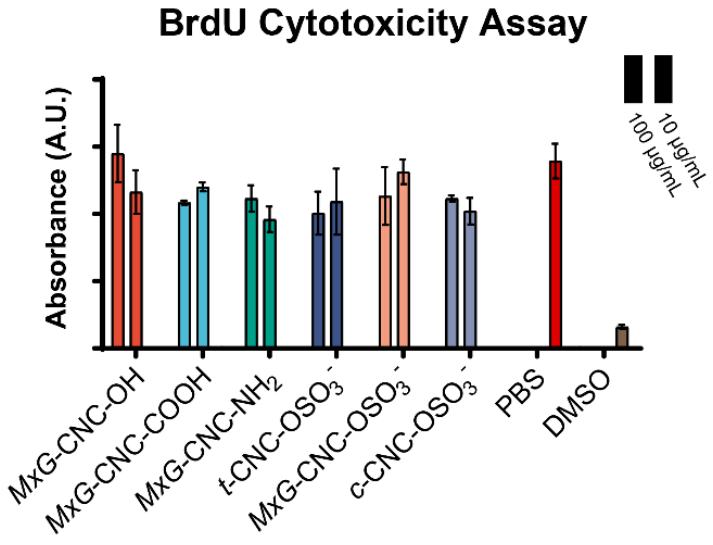

Figure S16: A BrdU ELISA was used to determine the effect of CNCs on cellular differentiation *in-vitro*. CNCs were incubated with RAW macrophages for 12 h, then BrdU reagent was added to cell culture media and incubated for an additional 12 h prior to conducting the assay.

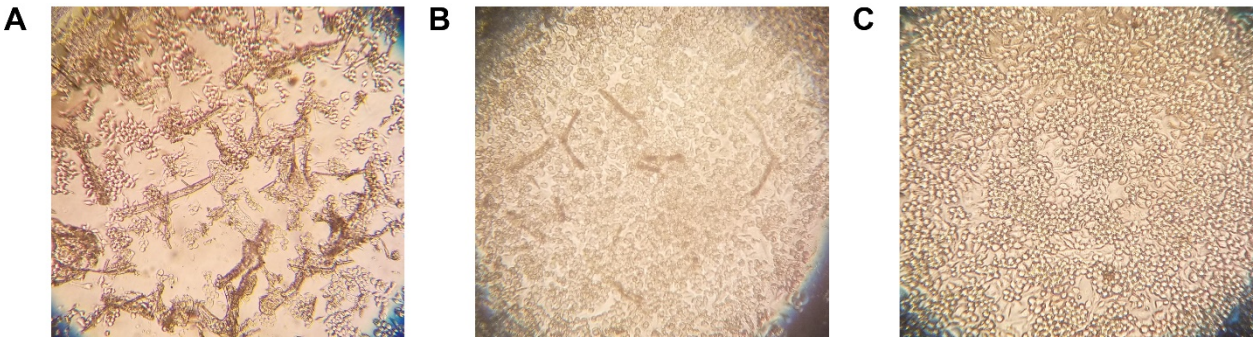

Figure S17: Light microscopy visualizing the presence of aggregates and disrupted cell growth in RAW-Blue cells incubated with A) *MxG*-CNC-OH samples but not with B) *MxG*-CNC-COOH or C) PBS control samples.

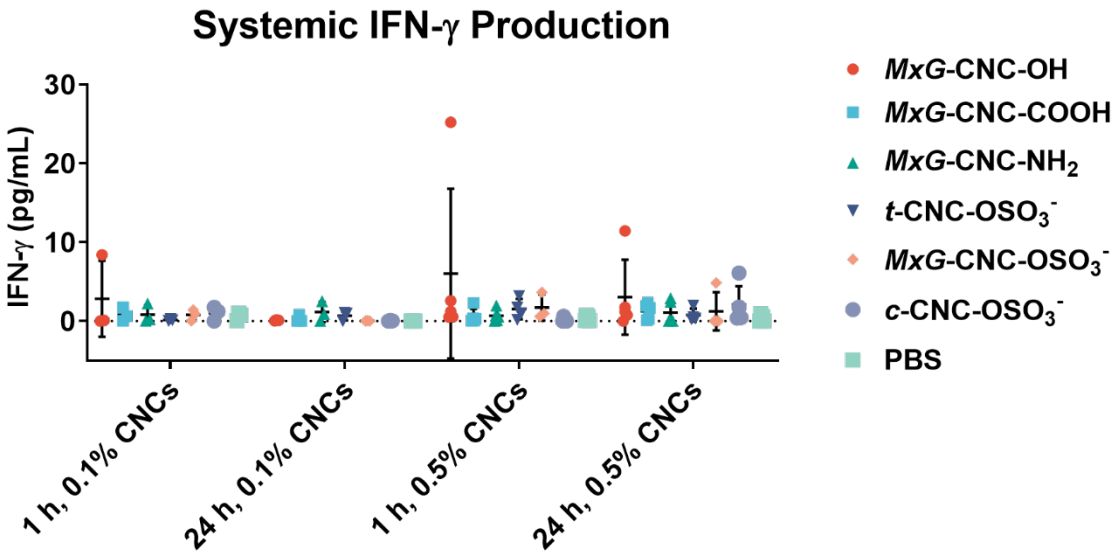

Figure S18: Systemic IFN-γ production was assayed 1 and 24 h after injection of CNCs using Mouse Inflammation CBA (BD Biosciences). No differences were observed between groups.

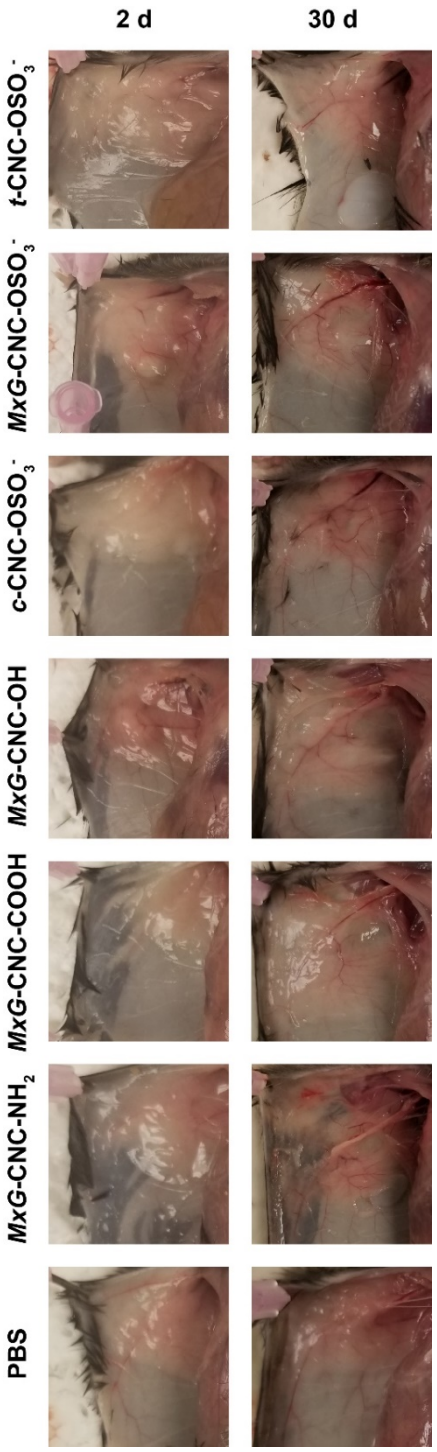

Figure S19: Images of subcutaneous tissue from the injection site were collected at the endpoint of the experiment. Imaging reveals redness in MxG-CNC-OH samples after 2 d but not 30 d. No significant inflammation is observed in other samples.

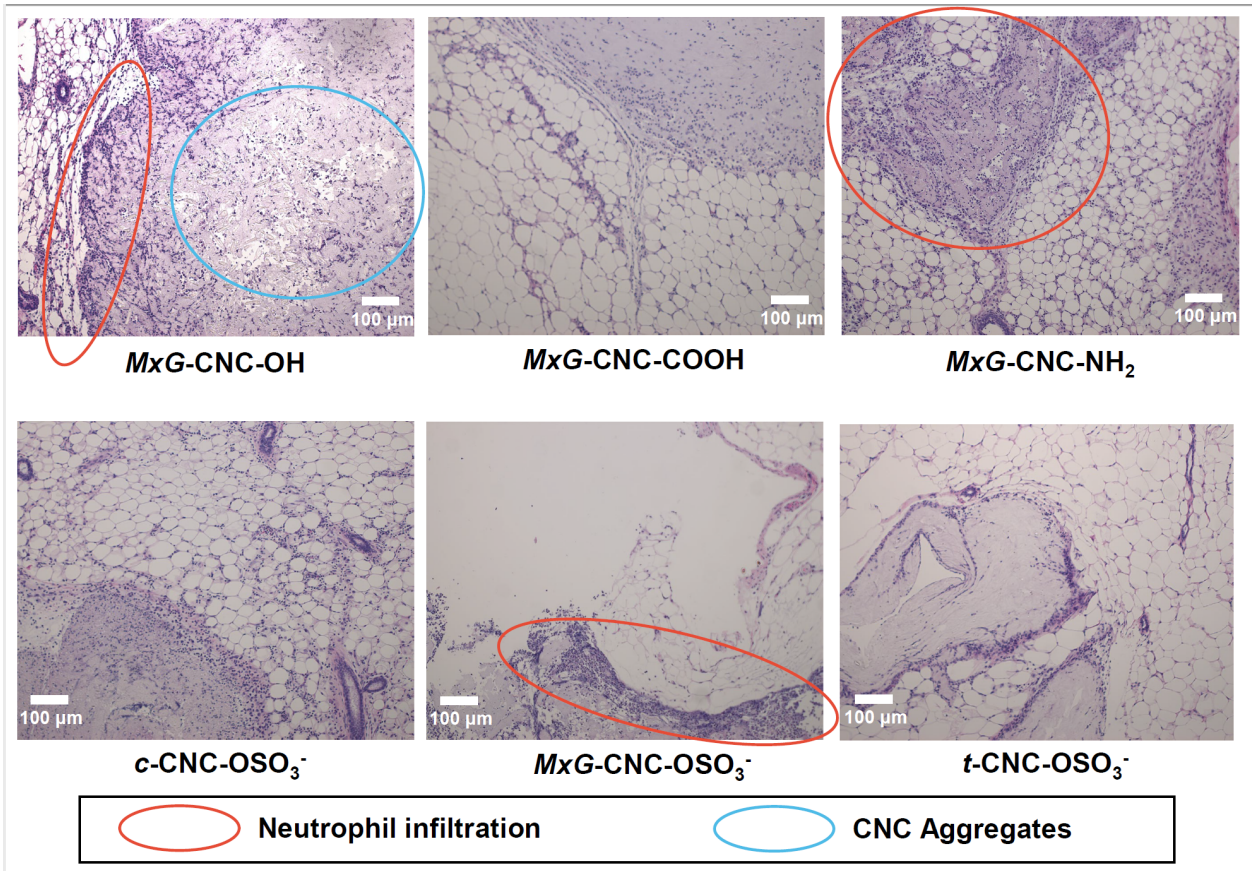

Figure S20: Hematoxylin and eosin staining of subcutaneous tissue collected from the injection site was conducted after 2 d for each of the CNCs analyzed *in-vivo* at a concentration of 0.5%. Significant neutrophil infiltration and presence of large aggregates were observed in the *MxG*-CNC-OH samples, suggesting an inflammatory response induced by these CNCs. Images of *MxG*-CNC-OH and *MxG*-CNC-COOH are duplicated from Figure 6 of the main text.

Supplementary References

S1. Jiang, F.; Esker, A. R.; Roman, M., Acid-catalyzed and solvolytic desulfation of H2SO4-hydrolyzed cellulose nanocrystals. *Langmuir* **2010**, 26 (23), 17919-17925.

S2. Way, A. E.; Hsu, L.; Shanmuganathan, K.; Weder, C.; Rowan, S. J., pH-Responsive Cellulose Nanocrystal Gels and Nanocomposites. *ACS Macro Lett* **2012**, 1 (8), 1001-1006.

S3. Park, S.; Baker, J. O.; Himmel, M. E.; Parilla, P. A.; Johnson, D. K., Cellulose crystallinity index: measurement techniques and their impact on interpreting cellulase performance. *Biotechnol Biofuels* **2010**, 3, 10.

S4. Flauzino Neto, W. P.; Silvério, H. A.; Dantas, N. O.; Pasquini, D., Extraction and characterization of cellulose nanocrystals from agro-industrial residue – Soy hulls. *Ind Crops Prod* **2013**, 42, 480-488.